

A&A manuscript no.
(will be inserted by hand later)
Your thesaurus codes are:
08.16.6; 02.18.5; 02.19.2

ASTRONOMY
AND
ASTROPHYSICS
8.6.2021

An inverse Compton scattering (ICS) model of pulsar emission

I. Core and conal emission beams

G.J. Qiao¹, W.P. Lin^{1,2}

¹ Department of Geophysics, Peking University, Beijing 100871, PRC.

² Beijing Astronomical Observatory, Chinese Academy of Sciences, Beijing 100080, PRC.

Received 18.7.1996; accepted 12.8.97

Abstract. Core and conal emission beams of radio pulsars have been identified observationally (Rankin 1983, 1993; Lyne and Manchester 1988). In the inner gap model (Ruderman and Sutherland 1975, hereafter RS75), the gap continually breaks down (sparking) by forming electron-positron pairs on a time scale of a few microseconds (RS75). This makes a large amplitude low frequency wave to be produced and which would be scattered by relativistic particles moving out from the gap. Under this assumption, Qiao (1988a, 1992) presented an Inverse Compton Scattering (ICS) model for both core and conal emissions. This paper presented a development of the model. Retardation and aberration effects due to different radiation components emitted from different heights are considered. The luminosity of pulsar radio emission via the ICS process is discussed. Coherent emission by bunches of particles is adopted and which is adequate to explain pulsar radiation. The theoretical results are in agreement with observations very well.

Key words: Radio pulsars: emission beams – radiation mechanism: inverse Compton scattering

1. Introduction

It's convincing that the emission beams of a radio pulsar can be divided into two (core, inner conal) or three (plus an outer conal) emission components through careful studies of the observed pulse profiles and polarization characteristics (Rankin 1983a, 1983b, 1986, 1990, 1993; Lyne & Manchester 1988). Many pulsar profiles at meter wavelength are dominated by core components. In usual polar cap models of pulsars, it is difficult to get a central or

“core” emission beam. Many current theoretical models can only get a hollow cone emission beams. Thus, it is needed to make an effort to get the core emission theoretically. Several authors such as Beskin et al. (1988), Qiao (1988a, b), Wang et al. (1989) presented some models for the core emission beam.

If the binding energy per ion in the neutron star surface is as large as 10 keV then ions will not be released, a pole magnetospheric vacuum gap (inner gap) is formed (RS75). More accurate variational calculations (e.g. Hillebrandt & Müller 1976; Flowers et al. 1977; Kössl et al. 1988) have revised downward the binding energy to a few keV. According to RS75, primary particles are accelerated to sufficient energies in the gap and emit high energy γ -quanta via curvature radiation (hereafter CR), which in turn, ignite pair production cascade to short out the acceleration potential (sparking). This is to say in the calculations for the cascade of the inner gap only CR process is taking into account. If the Inverse Compton Scattering (ICS) process in strong magnetic fields is taking into account the potential drops across the gap will be down, the “binding energy difficulty” will be released and the inner gap model (RS model) can still be sound, even if the binding energy downward to a few keV (Zhang and Qiao 1996, here after ZQ96; Qiao and Zhang 1996, here after QZ96; Zhang 1996; Zhang et al. 1997). The gap continually breaks down (sparking) by forming electron-positron pairs on a time scale of a few microseconds (RS75), this is inconsistent with the observed short-time scale structure (Hankins, 1992). A very large amplitude low frequency wave would be associated with the sparking, which would be scattered by relativistic particles moving out (if the low frequency wave can propagate in the magnetosphere of the neutron star, we will discuss this a little below). Under the assumption that the observed radio emission are produced by the ICS process of the high energy particles (secondary) off the low frequency waves, we can get

Send offprint requests to: W.P. Lin

both core and two conal components (Qiao 1988a,1992). The different emission components are emitted from different heights (Qiao et al. 1992, Lin and Qiao 94, hereafter LQ96, and this paper, see below).

In this paper we present a development of the work of Qiao (1988a,b;1992) which presented basic ideas and calculations for both core and two conal emission beams. Both observations (Rankin 1993) and the theory (Qiao, et al., 1992) show that the “core” emission is emitted at a place relatively close to the stellar surface, the “inner cone” is emitted at a lower height, and the “outer cone” is emitted at some greater height. If the different emission components are emitted at different heights, two effects, aberration and retardation effects, should be considered in the calculations. Our result shows that these effects move the apparent positions of the emission beams and change their shapes to be asymmetric to the magnetic axis. McCulloch (1992) examined about 20 triple profiles and found no example with the central component close to the leading component but many close to the trailing component, our calculations fit the result well. The basic idea, assumptions and the results of the calculations are presented in section 2; some theoretical respects and observational facts are discussed in sections 3.

This is one of a series papers about radio pulsar emission, on the polarizations both linear and circular, the behavior of pulse profiles in different frequencies, γ -ray emission and so on will be done later.

2. An inverse Compton scattering (ICS) model

2.1. Assumption

Along the line of RS inner gap model (RS75), Qiao (1988a,1992) presented a model for radio emission of pulsars. The basic assumptions of the model are as follows:

1. Neutron stars have dipole magnetic fields.
2. The Radio emission observed of pulsars is produced in an ICS process: a low frequency wave (with angular frequency $\omega_0 \sim 10^6 \text{s}^{-1}$) is scattered by high energy particles (with Lorentz factor $\gamma \sim 10^2 - 10^4$, this is the energy of the secondaries, see RS75 and if the ICS process of high energy particles off the thermal photon in or above the polar gap is taking into account, see Xia et al.1996, Bednarek et al. 1992, ZQ96, Luo 1996, Zhang et al. 1997). The low frequency wave is produced in the inner gap sparking (see RS75, the gap continually breaks down on a time scale of a few microseconds, the angular frequency is corresponding to $\omega_0 \sim 10^6 \text{s}^{-1}$, so the angular frequency $\omega_0 \sim 10^6 \text{s}^{-1}$ of the low frequency wave is taking in the calculation below). The high energy particles are the secondary particles produced near the gap (ZQ96 for self-consistent gap considering ICS-induced $\gamma - B$ process, also see Zhang et al. 1997 for discussion of three modes of pulsar inner gap).
3. The low frequency waves can propagate near the neutron stars. A possible reason for this may be that

large radiation pressure may make particle’s density along the path of the emission to be substantially less dense than that predicted (e.g. Sincell and Coppi 1996), and the plasma frequency should be much lower if nonlinear effects are taken into account (Chian and Clemow 1975).

2.2. The luminosity of the radio emission

The efficiency of the ICS process is higher than that of the CR process, but as the estimate below, incoherent radiation in ICS process is inadequate in explaining pulsar radiation either. We can write the luminosity of the ICS process as follows (see appendix):

$$L_{ics,incoh} = (1.5 \times 10^{33} \text{erg/s}) \zeta B_{12}^3 h_3^2 P^{-4} \gamma_3^2 (\sigma/\sigma_{th}) \quad (1)$$

here ζ is in order of 1, $B_{12} = B/(10^{12} \text{Gauss})$, B is the magnetic field near the surface of the neutron stars, h is the thickness of the gap, $h_3 = h/(10^3 \text{cm})$, P is the rotational period of the neutron star. σ is the cross section of the inverse Compton process, and σ_{th} is the Thomson cross section.

If we take $\sigma = \sigma_{th}/\gamma^2$ (see appendix), then

$$L_{ics,incoh} = (1.5 \times 10^{27} \text{erg/s}) \zeta B_{12}^3 h_3^2 P^{-4} \quad (2)$$

When the radiation take place at a higher position: for example, $r = 10R$, using $n_{ph} = n_{ph,0}(R/r)^3$, in this case we have:

$$L_{ics,incoh} = (1.5 \times 10^{24} \text{erg/s}) \zeta B_{12}^3 h_3^2 P^{-4} \quad (3)$$

The luminosity observed of radio pulsars can be written as (Sutherland 1979):

$$L = (3.3 \times 10^{25} \text{ergs/s}) S_{400} d^2 \quad (4)$$

where S_{400} is the mean flux density in mJy at 400MHz and d is the pulsar distance in kpc . The ranges of $S_{400} d^2$ is from ~ 10 to $\sim 10^5 mJy - kpc^2$. This means that incoherent ICS radiation is inadequate in explaining pulsar radiation. A coherent mechanism should be involved.

Coherent emission mechanisms may be classified as: (1). maser mechanisms; (2). a reactive or hydrodynamic instability; or (3). to emission by bunches. Theories for these coherent emission processes are not as well developed as theories for incoherent emission processes (Melrose 1992).

The emission mechanism suggested in this paper are favorable to the coherent emission by bunches. In the ICS process, the outgoing photons are produced in a scattering process: the low frequency wave is scattered by particles which is moving along a bunch magnetic field lines. In the process, the out going photons produced by particles of a bunch are coherent; and for those produced by particles in different sparking are not coherent. From this point of view, we can take a calculation to fit the linear and circular polarization observations of radio pulsars very well (Xu 1997; Qiao, Xu and Han 1997). If the number of the

particles in each sparking is N_i , the coherent luminosity of the ICS process is:

$$L_{ics,coh} = \sigma c n_{ph} \hbar \omega' \sum \left(\frac{dN_i}{dt} \right)^2 \quad (5)$$

where $\frac{dN}{dt} = \sum \left(\frac{dN_i}{dt} \right)$. If $\frac{dN_i}{dt} = \frac{dN_{i+1}}{dt}$, $\frac{dN}{dt} = n \left(\frac{dN_i}{dt} \right)$, then the ratio of coherent luminosity to incoherent luminosity is:

$$\eta = L_{ics,coh} / L_{ics,incoh} = n \left(\frac{dN_i}{dt} \right)^2 / \frac{dN}{dt} = \frac{dN_i}{dt} \quad (6)$$

Comparing Eq.(3) and (4), we find that $\frac{dN_i}{dt} \simeq 10^3 \sim 10^7$ is enough to produce observed radio emission. From $n_0 = n_{gj} \simeq \frac{\Omega \cdot \mathbf{B}}{2\pi c e}$ and $\frac{dN_i}{dt} = 2\chi\pi r_p^2 n_0 c$, we get

$$\frac{dN_i}{dt} = \frac{4\pi\chi B R^3}{c e P^2} = 2.7 \times 10^{30} \kappa B_{12} P^{-2} \quad (7)$$

where $r_p = R\theta_p = R\sqrt{2\pi R/Pc}$ is the radius of inner gap, and $R = 10^6 cm$ is the radius of the neutron stars. For typical parameters and $\kappa \simeq 1$, $\frac{dN}{dt}$ is about 10^{30} , this means that only few percentage (10^{-27} to 10^{-23}) of the coherent particles is enough to produce the observed radio emission.

For coherent curvature radiation, there is a fundamental weakness in existing theoretical treatments which do not allow for any velocity dispersion of the particles (Melrose 1992). In the mechanism discussed here the weakness is much weaker. This is because for the observed emission (including frequency and phase) is determined by the frequency of the incoming wave ω_0 , the energy of the particles (Lorentz factor γ) and the incoming angle θ_i , not only γ (see Eq.(8)).

2.3. The basic formulae for emission beams

For most pulsars, $B \ll B_q = 4.414 \times 10^{13} Gauss$ at the points near or far from the surface of neutron star. As Lorentz factor $\gamma \gg 1$, $\beta = v/c \simeq 1$, $\gamma\hbar\omega_0 \ll m_e c^2$ and $\theta' \sim 0$, in an ICS process of the outgoing high energy particles with the low frequency wave photons for the outgoing photons (with the energy of $\hbar\omega'$), we have (Qiao 1988a,b):

$$\omega' = \gamma^2 \omega_0 (1 - \beta \cos\theta_i)(1 + \beta) \simeq 2\gamma^2 \omega_0 (1 - \beta \cos\theta_i) \quad (8)$$

here, $\theta_i(\theta')$ is the incoming (outgoing) angle between the direction of motion of a particle and the incoming (outgoing) photon, m_e is the mass of electron, ω_0 is the angular frequency of the low frequency wave produced in the inner gap sparking. In the Lab frame, most of the outgoing photons are emitted along the direction of motion of a particle within a small beam which width is about γ^{-1} .

For a dipole magnetic field line, we have

$$r = R_e \sin^2 \theta \quad (9)$$

where r is the distance between a point Q and the center of the neutron star, $R_e = \lambda R_c$ ($\lambda \geq 1$), $R_c = Pc/2\pi$ is the radius of light cylinder, P is the pulse period of pulsar, R is the radius of the neutron star, θ is the polar angle at point $Q(r, \theta, \phi)$ with respect to the magnetic axis (see Fig. 1), $\lambda(\geq 1)$ is a constant for a dipole magnetic field line. For investigating the radiation, we only consider so-called open field lines.

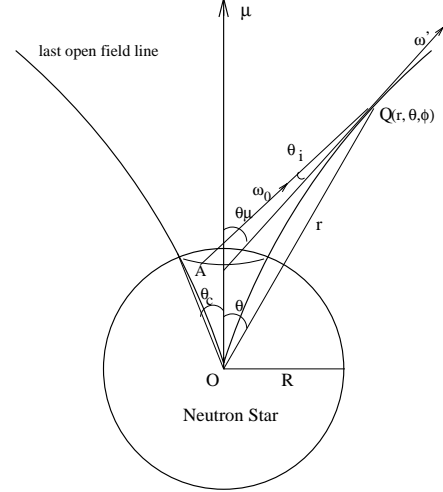


Fig. 1. Geometry for the inverse Compton scattering process. Low frequency waves are scattered by particles at point $Q(r, \theta, \phi)$. Dipole field line is assumed.

We consider the case that the low frequency wave is produced at the sparking point A near the boundary of the inner gap defined by the last open field lines. At any scattering point $Q(r, \theta, \phi)$ in a field line with R_e , the incident angle θ_i (see Fig. 1) can be written as follows,

$$\cos\theta_i = \mathbf{B} \cdot \mathbf{AQ} / (B \cdot AQ) \quad (10)$$

here, \mathbf{B} is the vector of magnetic field, \mathbf{AQ} is the direction vector of incoming low frequency wave.

In a right angle coordinate system a magnetic field can be written as:

$$\begin{cases} B_x = (B_r \sin\theta + B_\theta \cos\theta) \cos\phi - B_\phi \sin\phi \\ B_y = (B_r \sin\theta + B_\theta \cos\theta) \sin\phi + B_\phi \cos\phi \\ B_z = B_r \cos\theta - B_\theta \sin\theta \end{cases} \quad (11)$$

In a spherical coordinate system the dipole magnetic field will have components (Shitov,1985):

$$\begin{cases} B_r = \frac{m}{r^3} 2\cos\theta \\ B_\theta = \frac{m}{r^3} \sin\theta \\ B_\phi = 0 \end{cases} \quad (12)$$

and $B = \frac{m}{r^3} \sqrt{1 + 3\cos^2\theta}$. For the coordinate of point $A(x_a, y_a, z_a)$ and $Q(x_q, y_q, z_q)$, we have:

$$\begin{cases} x_a = R\sin\theta_c\cos\phi_c \\ y_a = R\sin\theta_c\sin\phi_c \\ z_a = R\cos\theta_c \end{cases} \quad (13)$$

$$\begin{cases} x_q = r\sin\theta\cos\phi \\ y_q = r\sin\theta\sin\phi \\ z_q = r\cos\theta \end{cases} \quad (14)$$

Then vector \mathbf{AQ} is:

$$\mathbf{AQ} = \{(x_q - x_a), (y_q - y_a), (z_q - z_a)\} \quad (15)$$

where the azimuthal angle ϕ ranges from 0 to 2π for different field lines which are symmetric to the magnetic axis, and $\theta_c = (2\pi R/ Pc)^{1/2}$ is the pole cap angle where the last open field line begins (see RS75), the azimuthal angle of the inner gap boundary ϕ_c can be from 0 to 2π .

With Eqs(8) to (13) we can get θ_i easily:

$$\cos\theta_i = M/N \quad (16)$$

where $M = 2r\cos\theta - R[3\cos\theta\sin\theta\sin\theta_c\cos(\phi - \phi_c) + (3\cos^2\theta - 1)\cos\theta_c]$, and $N = (1 + 3\cos^2\theta)^{1/2}\{r^2 + R^2 - 2Rr[\cos\theta\cos\theta_c + \sin\theta\sin\theta_c\cos(\phi - \phi_c)]\}^{1/2}$.

When the emission regions are far from the surface (that is for $r \gg R$, and $\theta_c \approx 0$) and in the plane of a field line (that is $\phi = \phi_c$), we have:

$$\cos\theta_i = \frac{2\cos\theta + (R/r)(1 - 3\cos^2\theta)}{\sqrt{(1 + 3\cos^2\theta)[1 - 2(R/r)\cos\theta + (R/r)^2]}} \quad (17)$$

The angle between the radiation direction (in the direction of the magnetic field) and the magnetic axis, θ_μ , has a simple relation with θ ,

$$ctg\theta_\mu = \frac{2ctg^2\theta - 1}{3ctg\theta} \quad (18)$$

The energy of high energy particles will be reduced when these particles come out along with the field lines owing to scattering with thermal photons and low frequency waves. It is assumed that:

$$\gamma = \gamma_0 [1 - \xi(r - R)/R_e] \quad (19)$$

where ξ reflects the energy lose of the particles and different pulsars have different γ_0 and ξ .

Using equations (8) to (19), we have a numerical relation between the outgoing photon frequency ω' and the beam radius θ_μ . In the coordinate system with magnetic axis as z axis, we have $\phi_\mu = \phi$. Finally, at any scattering point, we can get ω' and the radiation direction defined by θ_μ , ϕ_μ .

2.4. Retardation and aberration effects

Both observations (Rankin 1983a,b,1986,1990,1993; Lyne and Manchester,1988) and calculations (this paper and Qiao et al. 1992) show that the cone, ‘‘inner’’ cone and ‘‘outer’’ cone are emitted at different height (see Fig. 5), this makes the apparent beams move their positions relative to each other. Two points are considered in this paper: First, it needs time when the low frequency wave photons propagate to the points where they are scattered by relativistic particles. For the scattering process taking place at point $Q(r, \theta, \phi)$ (see Fig. 1), the emission point of the low frequency wave is not at point A , but at a point before that, as a result the incoming angle θ_i will be changed. In other words, for the scattering that takes place at this moment, the low frequency wave doesn’t come in from the present gap but the gap in an earlier position. The angle difference is $\Delta\theta = \Delta t/P \times 360^\circ$, where Δt is the time for light to travel between the point where the low frequency wave is emitted and the point where it is scattered. Secondly, the core and two cones are emitted at different heights, hence a time delay between them would change the apparent positions. Thus, we can get a new θ_i this makes that the beams are asymmetric to the magnetic axis: the central beam close to the trailing component of the cone, see Fig. 3.

2.5. Basic results

The calculation results are shown in the Figures. According to our calculated results, several main conclusions can be reached about the emission regions:

1. The theoretical emission beams we get have two or three parts, including ‘‘core’’ and ‘‘inner cone’’ and/or an extra ‘‘outer’’ cone at a given frequency. The angular radii of the beams are strongly related to the pulse period P and only P (see Fig. 2 and Fig. 3). This result is in good agreement with the empirical figure of double-conal geometry for some pulsars (Rankin 1993). The angular radius of central and conal beams are consistent with the conclusion from observations (Rankin 1983,1993). Fig. 2 shows emission beams for a slow rotating pulsar with period 1.0s, which have one core and double cones. Fig. 4 shows other emission beams for a fast rotating pulsar with $P \sim 0.1s$, which only have one core and one cone and it is very difficult to produce an ‘‘outer’’ cone for this kind of short-period pulsars.
2. These three different emission components are emitted at different heights (Fig. 5). The core emission is emitted at a place very close to the surface of the neutron stars in a ‘‘pencil’’ beam and the ‘‘inner’’ cone is emitted at a lower height along the same group of peripheral field lines where the ‘‘outer’’ cone is produced. This is to say that radio emission with the same frequency can be emitted at different heights along a

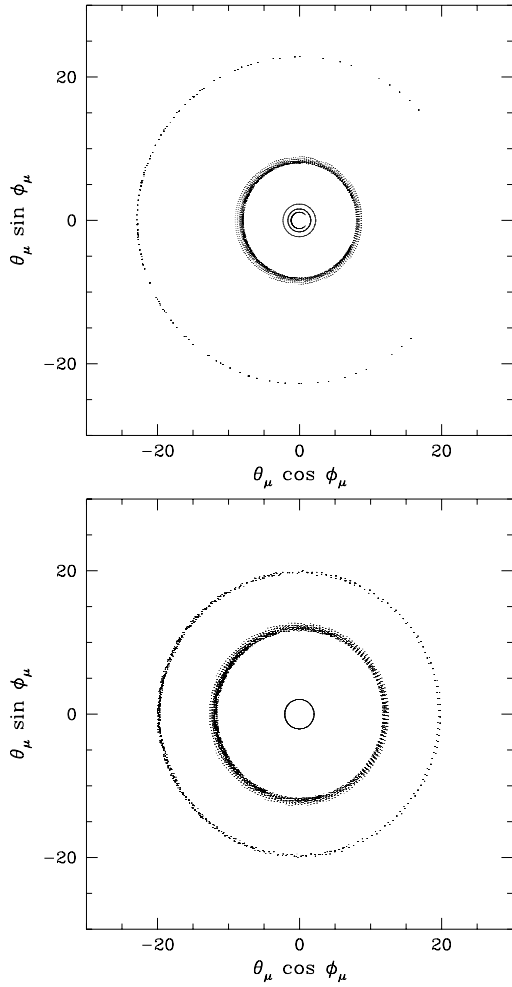


Fig. 2. Emission beams for a pulsar with $P = 1s$, $\alpha = 45^\circ$, $\gamma_0 = 10^3$, $\omega_0 = 10^6 s^{-1}$, $\xi = 1.0 \times 10^1$: **a.** at $350MHz$ (upper panel); **b.** at $500MHz$ (lower panel). The beams are slightly asymmetric to magnetic axis (which is perpendicular to the paper plane at the center of core). Retardation and aberration effects are weak for slow rotation pulsars.

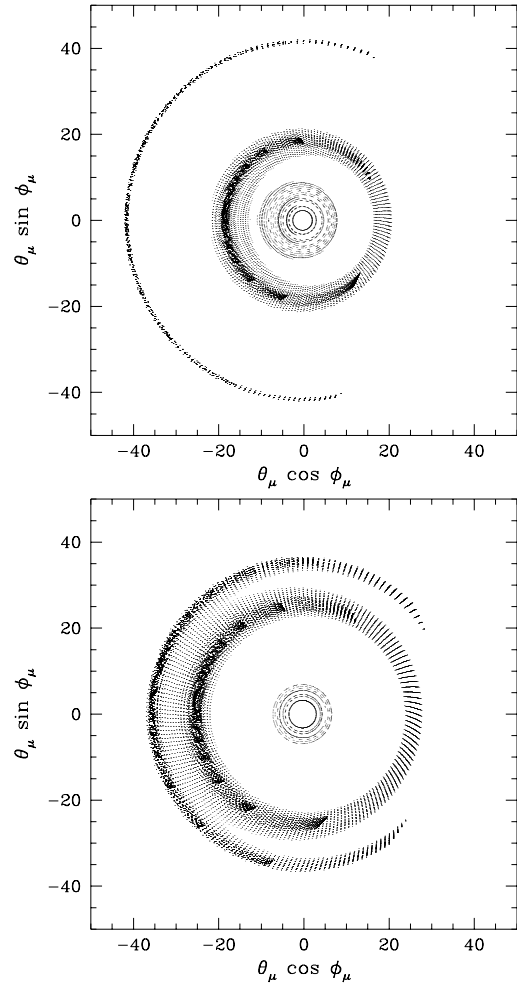


Fig. 3. Emission beams with obvious retardation and aberration effects: **a.** at $350MHz$ (upper panel); **b.** at $500MHz$ (lower panel). $P = 0.3s$, $\alpha = 45^\circ$, $\gamma_0 = 5 \times 10^2$, $\omega_0 = 10^6 s^{-1}$, $\xi = 5 \times 10^{-1}$. The beams are asymmetric to magnetic axis.

bunch of peripheral field lines, which is in agreement with the conclusion giving by Rankin (1993).

3. Considering the two effects of retardation and aberration, the theoretical beams for those pulsars with fast rotation will change their shapes. The apparent position of the core will move to later longitudes with respect to the position of the center of the cones.
4. In Fig. 6, at relatively low emission frequencies, core and inner cone can merge together (line B & line D) And at high frequencies, inner cone and outer cone, can merge together for slow rotating pulsars (line A). This can be seen clearly in Fig. 3.
5. In some case (Fig. 3 and Fig. 4), the leading part of outer cone can be broken.

3. Discussion and conclusion

3.1. Shape of emission beams and pulse profiles

The result in this paper shows that slow-rotation pulsars with long period such as $0.5s - 1.0s$ or longer, are “double-conal pulsars” with both inner and outer cone beams. This is in agreement with the conclusion given by Rankin (1993). Rankin’s table (1993) for **M** pulsars with five components shows, most of these 19 pulsars have long pulse periods. In the Fig. 6a, the opening angle (angular radius) becomes larger when the frequency increases (decreases) for the inner cone (outer cone). Fast pulsars, i.e. $P < 0.3s$, may only have a core and one inner conal emission component (Fig. 4 and Fig. 6b). For this class of pulsars, we suppose that observations tend to get triple (**T**) profiles. In Fig. 6b, as the frequency increases, the opening angle for the inner cone always increases. In this case, at higher frequency (from line D to line C), we will get a wider pulse

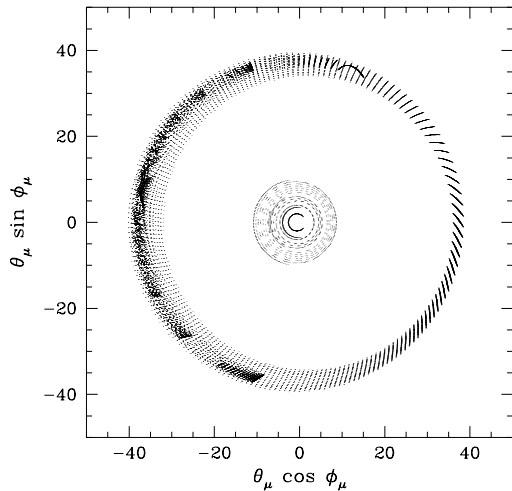


Fig. 4. Emission beams at 500MHz for a fast rotation pulsar with $P = 0.1\text{s}$, $\alpha = 45^\circ$, $\gamma_0 = 3 \times 10^2$, $\omega_0 = 10^6\text{s}^{-1}$, $\xi = 1 \times 10^{-1}$.

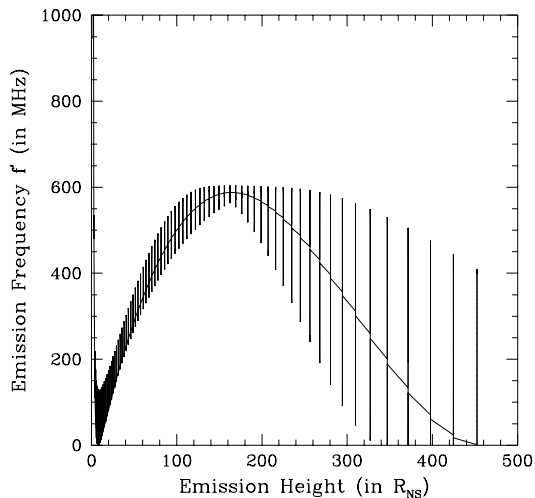


Fig. 5. A relation between the frequency and the emission heights for a pulsar with the same parameters of Fig. 2. When observing at a frequency, one should find that the core, inner cone and outer cone are emitted at different heights. The frequencies in the Figures in this paper only have relative meaning.

profile (Qiao 1992) in contrast to slow pulsars. This can be seen for some pulsars, such as PSR B1642-03 and PSR B1933+16 (Sieber et al. 1975).

We must mention that the theoretical angular radius of the outer conal beam is larger than in previous calculations and the height of the outer conal beam emission region is larger than that of Rankin's. This may be related to the parameter ξ in Eq.(5). A detailed calculation will show that the controller ξ is determined by the energy loss of particles, which depends on the strength of the

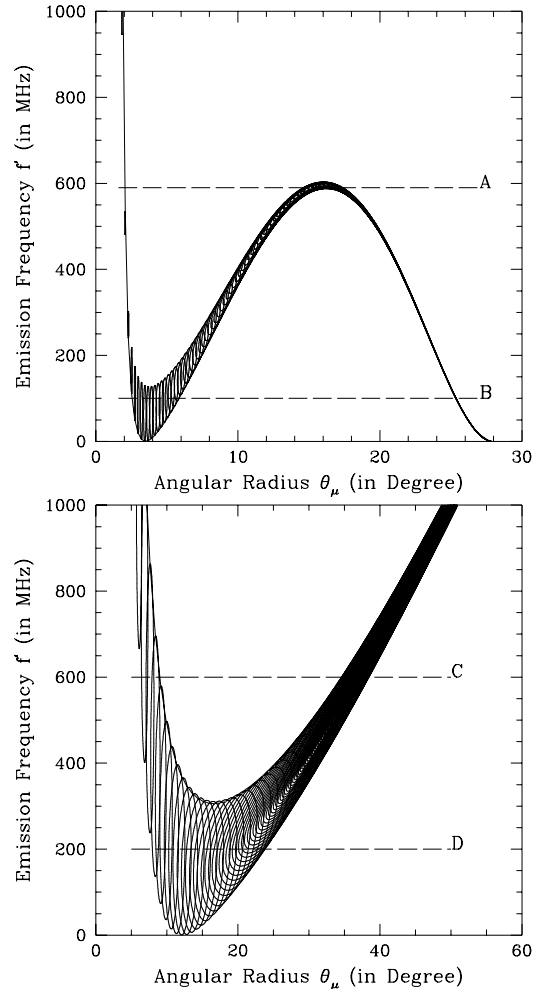


Fig. 6. Figure for $f' - \theta_\mu$ relation: **a.** with the same parameters of Fig. 2 (upper panel); **b.** with the same parameters of Fig. 4 (lower panel).

magnetic field and the thermal temperature at the surface of neutron stars (Zhang et al. 1997).

3.2. Does the “inner” cone radius increase as the observed frequency increases?

One result of this paper is that the inner cone radius increases as the observed frequency increases. This result is supported by analysis of observations. Wu et al.(1992) present a method to deal with the structure of the mean pulse profiles of pulsars. With that method and multi-frequency observational data, a diagram of $f' - \theta_\mu$ was given, which is very similar to the result of our calculation (see Fig. 6) and Fig.2 of Qiao (1992). Further analysis of Rankin (1993) did not emphasize that the angular radius of the inner cone ρ_{inner} increases when the frequency increases. More analysis of this is needed. A very direct method to check the result of this paper is that: for pulsars with “inner” and “outer” cone (five components), the

pulse profiles would become a triple (“inner” cone and “outer” cone get together) with a smaller central component at very high frequency (Fig. 6, line A); And also become a triple (the inner cone and core get together) with stronger central component at low frequency (Fig. 6, line B). This is in agreement with the observations, *e.g.* Izvekova et al. (1989).

3.3. conclusion

Our result shows, ICS process is a possible radiation mechanism for radio pulsars since it can produce the emission beams naturally and well consistent with observations. Rankin (1993) showed that the angular radii of core, “inner” cone and “outer” cone at a given frequency is a function of P (and only P !). This is just the result of the calculations in this paper. In agreement with the results given by Rankin (1993), we conclude that those pulsars only with “inner” cone (core single and triple in Rankin’s classification) are generally faster, those with “outer” cone (conal single and double) much slower, and the group of five-component (**M**) pulsars falls in between the other two. This paper also supports that the “inner” cone is emitted at a lower height along a same group of field lines that produce the “outer” cone. The shapes of pulse profiles change with frequencies in agreement with some kind of pulsars (Qiao 1992). The retardation and aberration effects induce asymmetry and can be observable, our result fits with observations (McCulloch 1992). These two effects may also change the linear polarization position angle (Xu, et al. 1996). The coherent emission of the ICS process suggested in this paper is an efficient mechanism to produce observed luminosity, and which is also a mechanism to produce observed polarization characters (Qiao et al. 1997).

Acknowledgements. We are very grateful to Professor M.A. Ruderman for his very impotent comments and suggestions. The authors thanks to Zhang B., Xu R.X., Han J.L., Gao K.Y. and Liu J.F. for helpful discussions. This work is partly supported by NSF of China, the Climbing Project-the National Key Project for Fundamental Research of China, and the Project supported by Doctoral Program Foundation of Institution of Higher Education in China.

Appendix

A. The efficiency of Curvature Radiation (CR) and the ICS processes

The energy loss of a particle through CR process is:

$$p_{cr} = \frac{2e^2 c \gamma^4}{3\rho^2} \quad (A1)$$

where γ is the Lorentz factor of the particles, e is the electric charge of the particles, c the light of speed, ρ is the radius of curvature of the magnetic field. The curvature radius ρ for dipole magnetic field is $\rho = \rho \sim \frac{4}{3}(rR_e)^{1/2}$, $R_e = \lambda R_c$, R_c is

the radius of the light cylinder, for last opening field lines the ρ is:

$$\rho = \rho \sim \frac{4}{3}(rR_c)^{1/2} \sim 10^8 cm P^{1/2} \quad (A2)$$

The energy loss of a particle through ICS is:

$$p_{ics} = \sigma c n_{ph0} \hbar \omega' \quad (A3)$$

where

$$\omega' \simeq 2\gamma^2 \omega_0 (1 - \beta \cos \theta_i) \quad (A4)$$

and σ is the total cross-section of ICS, n_{ph0} is the photon number density near the surface, $\hbar \omega'$ is the energy of the outgoing photons, near the surface, $\theta_i \simeq \pi/2$ and $\omega' \simeq 2\gamma^2 \omega_0$ can be taking in the estimate below, near the surface of the neutron stars, the photon number density can be written as:

$$n_{ph0} = \frac{s}{c \hbar \omega_0} \quad (A5)$$

$$s = \frac{c}{4\pi} E^2 \quad (A6)$$

where E is the electric field in the gap, as the inner gap sparking, one expects that the low frequency wave with electric field as the value of E . In the limit $h \ll r_p$ (h is the thickness of the gap, $r_p = R\theta_c$ is the radius of the gap), we have (RS75):

$$E = 2 \frac{\Omega B h}{c} \quad (A7)$$

Where B is the magnetic field near the surface of the neutron star. Substitute Eqs above to Eq.(A3), we have:

$$p_{ics} = \frac{2B^2 \gamma^2 h^2 \Omega^2 \sigma}{c\pi} \quad (A8)$$

So the ratio η of the energy loss of these two processes near the surface of the neuron star is:

$$\eta' = \frac{p_{cr}}{p_{ics}} = 0.8 \times 10^{-15} \gamma_3^2 P^2 B_{12}^{-2} h_3^{-2} \rho_8^{-2} \left(\frac{\sigma}{\sigma_{th}} \right)^{-1} \quad (A9)$$

If we use $\rho \sim 10^6 cm$ (RS75), the ratio η can be increase about 10^4 times, but η is still very small. This means that near the surface of the neutron star the efficiency of CR compare which the ICS is very low. Above the surface $\omega' \simeq \gamma^2 \omega_0$ can be taking, and

$$n_{ph} = n_{ph0} \left(\frac{R}{r} \right)^3 \quad (A10)$$

From the Eqs. above, we have:

$$\eta' = \frac{p_{cr}}{p_{ics}} = \frac{3\pi c^2 e^2 \gamma^2 r^2}{8R^3 B^2 h^2 \Omega^2 R_c \sigma} = 1.9 \times 10^{-5} \gamma_3^4 P r_8^2 B_{12}^{-2} h_3^{-2} \quad (A11)$$

where $\sigma \sim \gamma^2 \sigma_{th}$ (see below). Even if the typical radiation height is at $100 km$ in Eq.(A11), η' is still small. This means that the efficiency of the ICS process is higher than that of the CR process, but as the estimate bellow, the incoherent radiation of ICS process is inadequate in explaining pulsar radiation either.

B. Average number densities of the out flow

The energy flux carried by relativistic positrons into the magnetosphere above two polar gaps are (RS75):

$$\left(\frac{dE}{dt}\right)_{cur} = 2JdV\pi r_p^2 \quad (\text{B1})$$

where the current form in the magnetosphere is taken as (Sutherland, 1979):

$$J = J_{rot} + J_{\parallel} \quad (\text{B2})$$

here $J_{rot} = \rho(\Omega \times r)$, the current associated with the corotating plasma of charge density is (Goldreich and Julian 1969):

$$\rho_{gj} = \frac{\nabla \cdot \mathbf{E}}{4\pi} = -\frac{\Omega \cdot \mathbf{B}}{2\pi c} (1 - \Omega^2 r^2 \sin^2 \theta / c^2)^{-1} \quad (\text{B3})$$

If the magnetosphere is charge separated then the number density of the particles of charge is

$$n_0 = n_{gj} \simeq \frac{\Omega \cdot \mathbf{B}}{2\pi c e} \quad (\text{B4})$$

The second current corresponds to streaming of charges along the magnetic field lines: $j_{\parallel} = kB$, k must be constant along a given field line. This current only exist on the open field lines. The exact division between the open and closed field lines cannot be determined precisely. We may use the vacuum dipole field geometry to locate approximately the division on the neutron star and use the Eq.(B4).

If the potential in the inner gap has the maximum value (RS75):

$$dV = dV_{max} = \frac{\Omega B r_p^2}{2c} \quad (\text{B5})$$

We get

$$\left(\frac{dE}{dt}\right)_{cur} \simeq \left|\frac{dE}{dt}_{dip}\right| = \frac{2\Omega^4 R^6 B^2}{3c^3} \quad (\text{B6})$$

This means that the current flow from the gaps have enough braking torque on the spinning star and loss all the rotational energy (Sutherland 1979). This is reasonable, because $n_{gj} = n_+ - n_-$, Even if in the charge separated magnetosphere, n_0 can be much larger than the GJ density n_{gj} . Especially, in the place near the stellar surface. Near stellar surface, in the balance between the gravitational force and kinetic energy of the particles lets a thin atmosphere existence. We will estimate the luminosity of the ICS process using Eq.(B4).

C. Luminosity in incoherent ICS processes

The incoherent Luminosity by the ICS process near the surface of the neutron star is:

$$L_{ics, incoh} = \sigma c n_{ph} \hbar \omega' \frac{dN}{dt} \quad (\text{C1})$$

$$\frac{dN}{dt} = 2\chi \pi r_p^2 n_0 c \quad (\text{C2})$$

Substitute Eq.(A4)(B4) and (C2) to Eq.(C1), we can get the luminosities as follows:

$$L_{ics, incoh} = (1.5 \times 10^{33} \text{ erg/s}) \zeta B_{12}^3 \gamma_3^2 h_3^2 P^{-4} \left(\frac{\sigma}{\sigma_{th}}\right) \quad (\text{C3})$$

where ζ is in order of 1, σ_{th} is the Thomson cross section.

The ICS cross section σ for the low frequency discussed in this paper is (Qiao et al. 1986, Xia et al 1986) :

$$\sigma_T(1) = \sigma(1 \rightarrow 1') + \sigma(1 \rightarrow 2') \\ = \sigma_{th} \left\{ \sin^2 \theta + \frac{1}{2} \cos^2 \theta \left[\left(\frac{\omega}{\omega + \omega_B}\right)^2 + \left(\frac{\omega}{\omega - \omega_B}\right)^2 \right] \right\}^R \quad (\text{C4})$$

$$\sigma_T(2) = \sigma(2 \rightarrow 1') + \sigma(2 \rightarrow 2') \\ = \frac{1}{2} \sigma_{th} \left[\left(\frac{\omega}{\omega + \omega_B}\right)^2 + \left(\frac{\omega}{\omega - \omega_B}\right)^2 \right]^R \quad (\text{C5})$$

Here index ‘‘R’’ presents the parameters in the electron rest frame. In our case $\omega^R \ll \omega_B$, so $\sigma_T(1) \gg \sigma_T(2)$, and

$$\sigma_T(1) = \frac{\sin^2 \theta_i}{\gamma^2 (1 - \beta \cos \theta_i)} \sigma_{th} \quad (\text{C6})$$

where θ_i is the angle between the direction of the in coming photon and the magnetic field. As $\theta_i \simeq \pi/2$,

$$\sigma_T(1) \simeq \gamma^{-2} \sigma_{th} \quad (\text{C7})$$

or

$$\sigma_T(1)\omega' \sim \sigma_{th}\omega_0 \quad (\text{C8})$$

At the place $r \gg R$, we can use $n \simeq n_0 \left(\frac{R}{r}\right)^3$, if the radiation region is at $r = 100km$, so the luminosity in Eq.(C3) will be down 9 magnitude. The luminosity observed of radio pulsars can be written as (Sutherland,1979):

$$L = (3.3 \times 10^{25} \text{ ergs/s}) S_{400} d^2 \quad (\text{C9})$$

The ranges of $S_{400} d^2$ is from ~ 10 to $\sim 10^5 mJy - kpc^2$, which means that incoherent ICS radiation is inadequate in explaining pulsar radiation.

D. Coherent emission

See the text.

References

- Bednarek W., Cremonesi O. and Treves A., 1992, ApJ 390, 489
 Chian A.C.L. and Clemow P.C., 1975, J.Plasma Phys., 14, 505
 Goldreich P. and Julian W.H., 1969, ApJ, 157, 869
 Hankins T.H., 1972, ApJ, 177, L11
 Izvekova V.A., Kuz'min A.D., Malofeev V.M., & Shitov Y.P., 1989, J.Lebedev Physical Inst. 199, 13
 Lin W.P., Qiao G.J., 1994, in: Proceeding of 8th Guo Shoujing Summer School On Astrophysics, p.253 (LQ94)
 Lin W.P., 1995, Thesis for Master Degree, Peking University
 Luo Q., 1996, ApJ, 468, 338
 Lyne A.G. & Manchester R.N. 1988, MNRAS 234, 477
 McCulloch P.M., 1992, in: The Magnetospheric Structure and Emission Mechanisms of Radio Pulsars, eds. T.H. Hankins, J.M. Rankin and J.A. Gil, p.410

- Melrose D.B., 1992, in: *The Magnetospheric Structure and Emission Mechanisms of Radio Pulsars*, eds. T.H. Hankins, J.M. Rankin and J.A. Gil, p.307
- Qiao G.J., 1988a, in: *Vistas in Astronomy* 31, 393
- Qiao G.J., 1988b, in: *High Energy Astrophysics*, eds. G. Borner, New York, Springer-Verlag, p.88
- Qiao G.J., 1992, in: *The Magnetospheric Structure and Emission Mechanisms of Radio Pulsars*, eds. T.H. Hankins, J.M. Rankin and J.A. Gil, p.239
- Qiao G.J., Li C.G., and Li M., 1992, in: *The Magnetospheric Structure and Emission Mechanisms of Radio Pulsars*, p.243
- Qiao G.J., Wu X.J., Bao W. and Xia X.Y., 1986, *Scientia Sinica*, 1986, 7, 732
- Qiao G.J. and Zhang B., 1996, *A&A*, 306, L5. (QZ96)
- Qiao G.J., Zhang B., Lin W.P., 1994, in: *Proceedings of the First Sino-Indian School On Astronomy & Astrophysics*, in press
- Qiao G.J., Xu R.X. and Han J.L., 1997, in preparing
- Rankin J.M., 1983b, *ApJ*, 274, 359
- Rankin J.M., 1986, *ApJ*, 301, 901
- Rankin J.M., 1988, *ApJ*, 325, 314
- Rankin J.M., 1990, *ApJ*, 352, 247
- Rankin J.M., 1993, *ApJ*, 405, 285
- Rankin J.M., 1993, *ApJS*, 85, 145
- Ruderman M.A., Sutherland P.G., 1975, *ApJ*, 196, 51 (RS75)
- Shitov Yu.P., 1985, *Sov.Astron.* 29, 33
- Sieber W., Reinecke R., and Wielebinski R., 1975, *A&A* 38, 169
- Sincell M.W. & Coppi P.S., 1996, *ApJ*, 460, 163
- Sutherland P.G., 1979, *Fundamentals of Cosmic Physics*, 1979, 4, 95
- Wang D.Y., Wu X.J., Chen H., 1989, *Ap&SS*, 161, 271
- Xia X.Y., Qiao G.J. and Wu X.J., 1986, *Acta Astrophysica Sinica*, 6, 160
- Wu X.J., Xu W., Rankin J.A., 1992b, in: *The Magnetospheric Structure and Emission Mechanisms of Radio Pulsars*, eds. T.H. Hankins, J.M. Rankin and J.A. Gil, p.172
- Xu R.X., 1997, PhD thesis, Peking University
- Xu R.X., Qiao G.J. & Han J.L., 1996, in: *Proceedings of IAU Colloquium No.160*, eds. S. Johnston et al., p.183
- Zhang B., Qiao G.J., 1996, *A&A*, 310, 135 (ZQ96)
- Zhang B., Qizo G.J., Lin W.P. and Han J.L., 1997, *ApJ*, 478, 313
- Zhang B., Qizo G.J. and Han J.L., 1997, submitted to *ApJ*